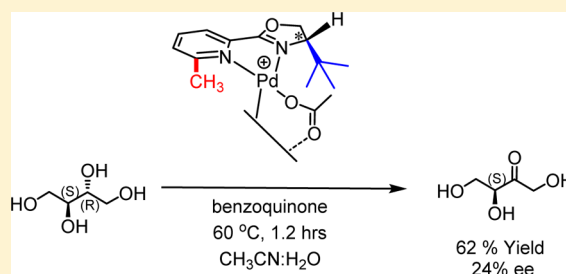


Chemoselective Oxidation of Polyols with Chiral Palladium Catalysts

Antonio G. De Crisci,[†] Kevin Chung,[†] Allen G. Oliver,[‡] Diego Solis-Ibarra,[†] and Robert M. Waymouth^{*†}[†]Department of Chemistry, Stanford University, Stanford, California 94305, United States[‡]Molecular Structure Facility, Department of Chemistry and Biochemistry, University of Notre Dame, Notre Dame, Indiana 46556, United States

Supporting Information

ABSTRACT: Chiral palladium-based catalysts derived from pyridinyl oxazoline (pyOx) ligands catalyze the oxidation of alcohols, including 1,2-diols, triols, and tetraols, with high regio- and chemoselectivity. Screening of various chiral oxazoline-derived ligands for the oxidation of a model diol, 1,2-propanediol (1,2-PD), revealed that the nature of the ligand had a significant influence on the activity and chemoselectivity for oxidation of vicinal diols. The PyOx ligands containing an α -methyl substituent were the most active for the oxidation of 1,2-PD using benzoquinone as the terminal oxidant. Oxidation of vicinal diols and polyols occurs selectively at the secondary alcohol to afford α -hydroxy ketones in isolated yields of 62–87%. Chemoselective oxidation of *meso*-erythritol with the chiral [(*S*)-(α -Me(*tert*-Bu)PyOx)Pd(OAc)]₂[OTf]₂ afforded (*S*)-erthryulose in 62% yield and 24% ee.



INTRODUCTION

The oxidation of alcohols to carbonyl compounds is one of the most widely used synthetic transformations.^{1–6} Selective catalytic oxidations are environmentally attractive alternatives to those utilizing stoichiometric heavy-metal oxidants.^{6–11} Palladium-catalyzed oxidations have proven attractive due to the mild conditions, high chemo-^{12–14} and stereoselectivities,^{3,15–17} and the use of air or oxygen as terminal oxidants.^{18–30}

We recently reported that cationic Pd complexes^{12,31–33} ligated by neocuproine (2,9-dimethylphenanthroline)^{7,18} ligands catalyze the chemoselective oxidation of vicinal diols and triols to α -hydroxy ketones at room temperature.¹² α -Hydroxy ketones are versatile synthetic intermediates and a common functional group in biologically active natural products;^{34–37} the chemoselective oxidation of vicinal diols to hydroxy ketones provides a mild and selective strategy to these intermediates.

Cationic Pd acetate complexes ligated by phenanthrolines substituted in the 2- or 2,9-positions are active catalysts for the oxidation of primary or secondary alcohols^{31–33} and vicinal diols¹² at room temperature. Cationic monoacetate complexes were more active than either the dicationic complexes³¹ or the diacetates;^{38,39} we have reasoned that the presence of both an acetate ligand and exchangeable cationic coordination site facilitates ligand exchange and deprotonation of the alcohol to generate cationic Pd alkoxides.^{31–33} The presence of 2,9-substituents on the phenanthroline ligands is critical; Pd complexes ligated by unsubstituted phenanthrolines are inactive at room temperature.³¹

Herein, we describe efforts to develop chiral Pd complexes for chemo- and enantioselective polyol oxidation reactions and describe features of the ligand geometry which influence both

the catalytic activity and chemoselectivity for diol and polyol oxidation.

RESULTS AND DISCUSSION

Synthesis. To expand the scope of catalysts for chemo- and stereoselective alcohol oxidation, we targeted cationic Pd complexes ligated by chiral oxazoline ligands,^{40–45} including the chiral bis(oxazoline) *tert*-BuBOX (L1),^{40,46} the bi(oxazolines) L2a,b,^{41,47,48} and the pyridinyl oxazolines (pyOx) L3a–d (Figure 1).^{44,49–55}

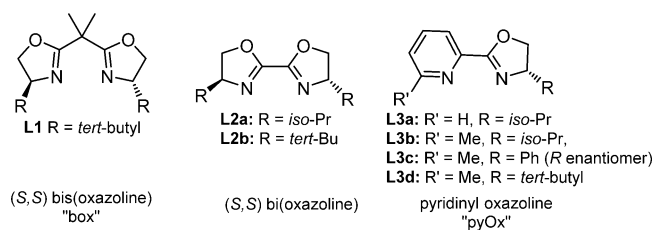


Figure 1. Oxazoline ligands.

The chiral bis(oxazoline) *tert*-BuBox (L1) is commercially available; the syntheses of the bi(oxazolines) L2a,b were carried out following literature protocols.⁴⁶ The syntheses of the pyOx ligands L3a–d were carried out using slightly modified literature procedures^{50,56,57} from commercially available β -amino alcohols and substituted 2-pyridinecarbonitriles.

To assess the suitability of the chiral ligands for low-temperature alcohol oxidation, screening studies were carried

Received: February 25, 2013

Published: March 21, 2013

out with cationic Pd complexes either isolated or generated in situ³¹ with ligands L1–L3. For these studies, the Pd acetate complex (L1)Pd(OAc)₂ and dicationic complex [(L1)Pd(MeCN)₂][BF₄]₂ were generated by reaction of a dichloromethane solution of the dichloropalladium complex (L1)-PdCl₂⁵⁸ with AgOAc or AgOTf/CH₃CN, respectively. Attempted oxidation of 1,2-propanediol in DMSO-*d*₆ with 2 equiv of benzoquinone (25 °C) with the product resulting from combining^{31,33} (L1)Pd(OAc)₂ and [(L1)Pd(MeCN)₂][BF₄]₂ was unsuccessful. Subsequent analysis of the reaction product by ¹H NMR and electrospray ionization mass spectrometry (ESI-MS) revealed that the reaction of (L1)Pd(OAc)₂ and [(L1)Pd(MeCN)₂][BF₄]₂ generated the palladacycle [(L1[∧]C)-Pd(MeCN)]⁺ resulting from carbometalation of one of the *tert*-butyl groups of L1. This was established by the observation of characteristic ions at *m/z* 443.1695 [(L1[∧]C)Pd(CD₃CN)]⁺ and *m/z* 399.1236 [(L1[∧]C)Pd]⁺ in the HR-MS desorption ESI (DESI; see the Supporting Information) and by diastereotopic CH₂ peaks at 2.13 ppm (qd, *J* = 9.0, 1.2 Hz) and the *tert*-butyl group derived diastereotopic methyl groups at 0.95 (d, *J* = 1.2 Hz) and 0.93 ppm in CD₃CN solution. The cyclopalladation of *t*-Bu-substituted oxazolines has been observed previously.⁵⁹ DFT computations (M06-L) of [(L1[∧]C)Pd(MeCN)]⁺ (Figure 2; see the Supporting Informa-

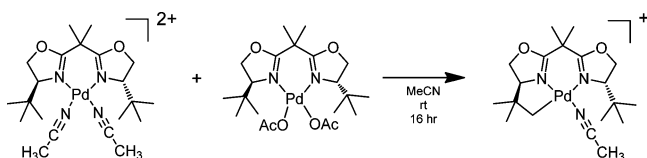


Figure 2. Observed C(sp³)-H activation of L1 upon comproportionation, characterized by ¹H NMR, ¹³C NMR including DEPT135, and HR-MS (DESI). See the Supporting Information.

tion) indicate that the palladacycle adopts a puckered five-membered ring with the C(Me)₂ moiety out of plane. The nitrogen trans to the Pd–C bond is longer by 0.21 Å at 2.22 Å in comparison to the Pd–N trans to the acetonitrile.

Reasoning that the conformational flexibility of the bis(oxazoline) ligand L1⁶⁰ might have contributed to the undesired ligand carbometalation, we investigated the related bi(oxazoline) ligands (L2a,b) which adopt more planar five-membered chelates with Pd.^{61,62} Nevertheless, when (L2a)Pd(OAc)₂ and [(L2a)Pd(CH₃CN)₂](OTf)₂ were combined in CH₃CN and left to react for 1 h at room temperature, analysis of the resulting mixture by MS (ESI) revealed ions at *m/z* 370.12 and 329.14, consistent with the cyclopalladated metallacycles [(L2a[∧]C)Pd(MeCN)]⁺ and [(L2a[∧]C)Pd]⁺, respectively.

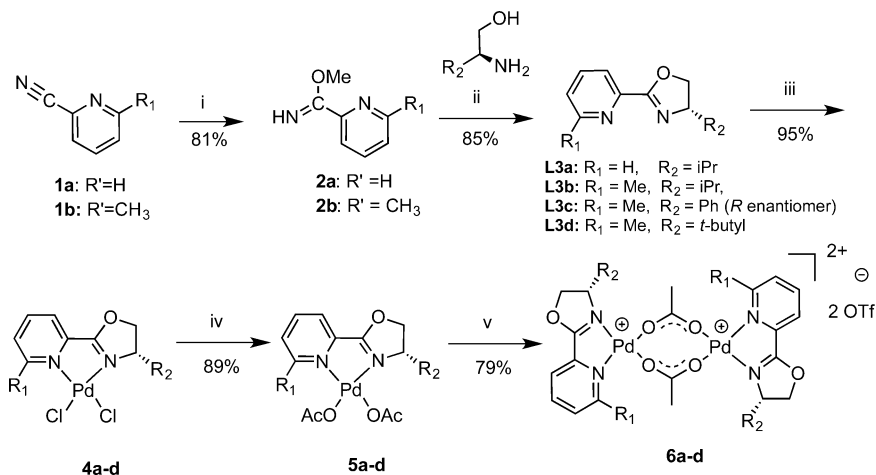
Attempts to generate a cationic Pd acetate in situ³² by treating (L2a)Pd(OAc)₂ with 1 equiv of HOTf (to Pd, as a 0.33 M MeCN solution) was similarly unsuccessful; this mixture was inactive for oxidation of 1,2-propanediol (2 equiv of benzoquinone) after 16 h at 25 °C in DMSO-*d*₆.

More promising reactivity was observed with the *tert*-butyl-substituted ligand L2b when an external base was added. When [(L2b)Pd(CH₃CN)₂](BF₄)₂ (prepared by reaction with L2b and [(MeCN)₄Pd][BF₄]₂) was combined with 0.5 equiv of Cs₂CO₃ or CsOAc (relative to Pd), 1,2-propanediol, and benzoquinone in DMSO-*d*₆, hydroxyacetone was observed after heating at 40–60 °C for 2 days, although under these conditions, the yields were modest (≤23%) and Pd black also formed. Similarly, oxidation of 1,2-propanediol with [(L2b)Pd(CH₃CN)₂](BF₄)₂ activated with 1 equiv of aqueous NaOH⁶³ afforded a 19% yield of hydroxyacetone after 16 h at 60 °C in DMSO-*d*₆.

In light of the modest activities observed with ligands L1 and L2, we investigated the activity of Pd complexes of the pyOx ligands L3. Complexes 6a–d were prepared as shown in Scheme 1.

Initial screening of complex 6a by ¹H NMR revealed it to be inactive at room temperature for the oxidation of 1,2-propanediol with 10 mol % Pd and 1.15 equiv (relative to diol) of benzoquinone in DMSO-*d*₆ or 9/1 CD₃CN/D₂O mixtures. Higher conversions (29% at 2 h) was observed at 60 °C to afford a 12% yield of hydroxyacetone. As the reaction progressed to 17 h, conversion increased to approximately 60%

Scheme 1. Representative Synthesis of [(RPyOX)Pd(OAc)]₂²⁺(OTf)₂ with Conditions and Yields Reported for 6d (Dimer Shown)^a



^aLegend: (i) NaOMe, MeOH, 4 h, room temperature; (ii) (*S*)-2-amino-3,3-dimethyl-1-butanol (*L-tert*-leucinol), neat, 50 °C, Ar purge; (iii) (PhCN)₂PdCl₂, dichloromethane, 18h, room temperature; (iv) AgOAc, dichloromethane (dark), 45 min, room temperature; (v) MeCN/HOTf solution, 40 min, room temperature.

but the yield of hydroxyacetone dropped to 9% accompanied by the formation of Pd black.

As previous studies with phenanthroline-type ligands had indicated that α -methyl substitution was beneficial,^{12,31–33} we prepared the methylpyridine complexes **6b–d**. ¹H NMR screening experiments of complexes **6b–d** revealed these complexes to be more active and selective than those derived from **6a**; oxidation of 1,2-propanediol with **6b** afforded 37% of hydroxyacetone and 7% of lactaldehyde (NMR vs internal standard and 2 equiv of BQ in DMSO-*d*₆) after 8 h at room temperature. Similarly, oxidation of 1,2-propanediol with **6c** afforded 23% of hydroxyacetone after 13 h at room temperature with 2 equiv of BQ. Complex **6d** gave the most promising rates and selectivity: oxidation of 1,2-propanediol in CD₃CN/D₂O (9/1) with 10 mol % Pd and 2 equiv of benzoquinone at 55 °C led to complete conversion of diol and formation of 1-hydroxyacetone with 99% selectivity in less than 45 min. These screening studies revealed that, for oxidation of diols with the pyOx ligands, the presence of both an α -methyl substituent on the pyridine and a *t*-Bu substituent on the oxazoline were optimal for high rates and selectivities. In light of these promising results, preparative oxidation reactions were carried out with complex **6d**. In addition, complexes **4c,d** and **6a,d** were characterized by X-ray crystallography.

The synthesis of complexes **4–6** is summarized in Scheme 1; the synthesis of **6d** is described in detail below. Palladation of ligand **L3d** with Cl₂Pd(PhCN)₂ in dichloromethane afforded the dichloride **4d** in 95% yield. Treatment of **4d** with AgOAc afforded the diacetate, which was subsequently converted to **6d** by treatment with 1 equiv of triflic acid.³² Attempts to generate **5d** directly from ligand **L3d** and Pd(OAc)₂ in refluxing toluene or benzene led to mixtures which were not readily purified. It is known that pyBox ligands are susceptible to nucleophilic ring opening from acetate attack⁶⁴ and may be responsible for the failure to generate **5d** directly from Pd(OAc)₂. Complex **5d** has limited stability and was converted to **6d** on the same day it was made to prevent decomposition. A similar observation was reported by Yoo with pyOx Pd acetates.⁵² Complex **6d** is obtained in 86% yield as its bridging dimer after precipitation with diethyl ether to give an air-stable orange precipitate. We note that **6d** is stable for at least several days (more stable than **5d**) at room temperature when protected from light with aluminum foil (taken as a precaution).

The single-crystal X-ray structure of **4c** is shown in Figure 3. The complex crystallizes as dark orange blocklike crystals from slow evaporation in a concentrated chloroform-*d* solution at room temperature. The Pd is coordinated in a distorted four-coordinate square-planar geometry by two chlorine atoms and the two nitrogens of the *R* enantiomer of the pyOx ligand **L3c**.

The palladium–nitrogen distances are Pd1–N1 = 2.003(2) and Pd1–N2 = 2.131(2) Å. The pyridyl Pd–N distance is 0.104 Å longer in **4c** than in the nonmethylated analogue reported by Jones et al.,⁶¹ likely as a consequence of the steric demands of the methyl group. The presence of an α -methyl group is also evident in the Cl–Pd–N angles, N2–Pd1–Cl1 = 169.8° and N1–Pd1–Cl2 = 177.27° for **4c**, in comparison to the nonmethylated version, 173.07 and 173.02°,⁶¹ revealing a larger deviation along the angle defined at the pyridine nitrogen of **4c**.

A single-crystal X-ray structure of **4d** was also obtained and is shown in Figure 4. The complex crystallizes as yellow blocklike crystals from a red dichloromethane/hexane solution at room temperature. The Pd is coordinated in a distorted four-

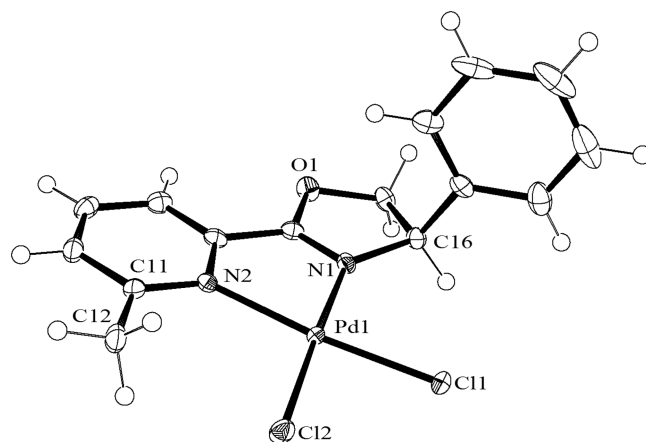


Figure 3. Single-crystal X-ray structure of **4c**. Ellipsoids are drawn at the 50% probability level. The solvent molecule is omitted for clarity. Relevant bond distances (Å) and bond angles (°): Pd1–N1, 2.003(2); Pd1–N2, 2.131(2); Pd1–Cl1, 2.280(1); Pd1–Cl2, 2.307(2); N2–Cl1, 1.349(3); C11–C12, 1.488(3); N1–Pd1–N2, 79.7(1); N1–Pd1–Cl1, 90.35(5); N2–Pd1–Cl1, 169.8(1); N1–Pd1–Cl2, 177.27(5); N2–Pd1–Cl2, 102.5(1); Cl1–Pd1–Cl2, 87.39(2); N1–C16–C2, 111.0(1); N1–C16–C8, 101.0(2); C11–N2–Pd1, 132.0(1); C10–N2–Pd1, 111.1(1).

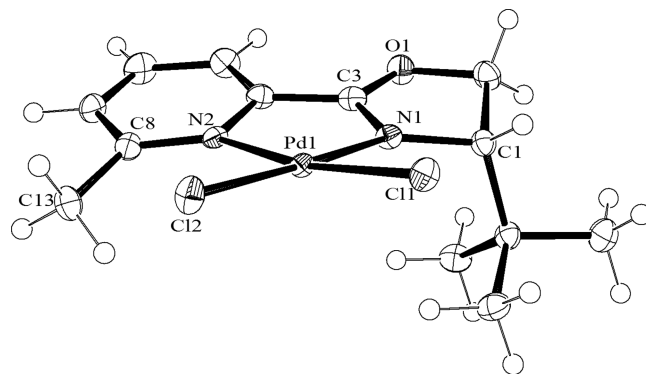


Figure 4. Single-crystal X-ray structure of **4d**. Ellipsoids are drawn at the 50% probability level. The dichloromethane solvent molecule is omitted for clarity. Relevant bond distances (Å) and bond angles and torsion angles (°): Pd1–N1, 2.001(2); Pd1–N2, 2.112(2); Pd1–Cl1, 2.2786(6); Pd1–Cl2, 2.2900(6); N1–Pd1–N2, 80.08(9); N1–Pd1–Cl1, 91.29(7); N2–Pd1–Cl1, 169.05(6); N1–Pd1–Cl2, 177.64(6); N2–Pd1–Cl2, 99.98(6); Cl1–Pd1–Cl2, 88.37(2); N2–Pd1–N1–C3, 16.13(19); Cl1–Pd1–N1–C3, –157.09(19); Cl2–Pd1–N1–C3, –75.6(17); N2–Pd1–N1–C1, –169.5(3); Cl1–Pd1–N1–C1, 17.3(3); Cl2–Pd1–N1–C1, 98.8(16).

coordinate square-planar geometry by two chlorine atoms and the two nitrogens of the pyOx ligand. The distortion evident in the N2–Pd1–Cl1 angle of 169.05(6)° is likely due to the steric demands of the *tert*-butyl substituent of the oxazolinyl ligand. Similar distortions have been noted previously;²⁷ Yoo and co-workers⁵² reported the X-ray structure for a compound analogous to **4d**, lacking an α -methyl substituent on the pyridine. Introduction of the α -methyl substituent causes a slight lengthening of the Pd1–N2 bond of **4d** (2.11 vs 2.05 Å for the complex⁵² lacking this substituent).

Single crystals of **6a** were obtained as yellow needlelike blocks from an acetonitrile/diethyl ether solution at room temperature. The dimeric dication crystallizes in space group C222₁ and is shown in Figure 5. The Pd–N pyridyl bond lengths are approximately 2.01 Å, while those of the oxazolyl

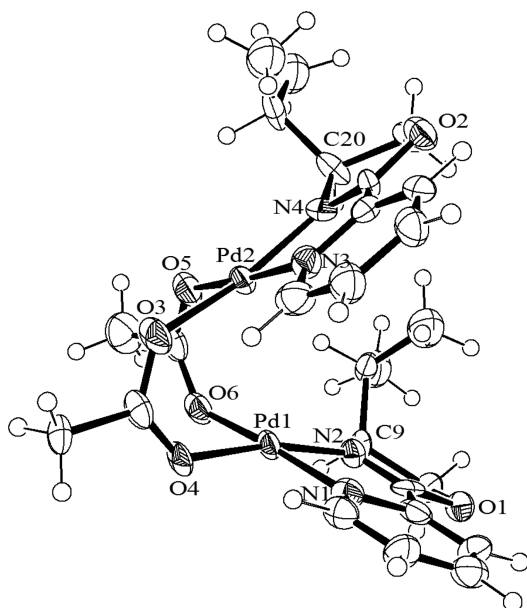


Figure 5. X-ray structure of the bridging acetate dimer **6a**. The two triflate counterions are omitted for clarity. Ellipsoids are drawn at the 50% probability level. Selected bond distances (Å) and bond angles ($^{\circ}$): Pd1–Pd2, 3.0742(9); Pd1–O6, 1.986(7); Pd1–N2, 1.987(8); Pd1–O4, 2.011(6); Pd1–N1, 2.012(8); Pd2–N4, 1.997(9); Pd2–O3, 2.001(7); Pd2–O5, 2.019(7); Pd2–N3, 2.022(9); O4–Pd1–N, 194.1(3); O6–Pd1–Pd2, 79.8(2); N2–Pd1–Pd2, 113.7(2); O4–Pd1–Pd2, 77.4(2); N1–Pd1–Pd2, 106.3(2); N4–Pd2–O3, 168.3(3); N4–Pd2–O5, 95.0(3); O3–Pd2–O5, 91.3(3); N4–Pd2–N3, 80.5(4); O3–Pd2–N3, 92.9(3); O5–Pd2–N3, 175.3(3); N4–Pd2–Pd1, 112.8(2); O3–Pd2–Pd1, 78.3(2); O5–Pd2–Pd1, 76.2(2); N3–Pd2–Pd1, 106.8(2); O6–Pd1–N2, 95.3(3); O6–Pd1–O4, 89.1(3); N2–Pd1–O4, 168.6(3); O6–Pd1–N1, 173.7(3); N2–Pd1–N1, 80.6(3).

Pd–N are approximately 1.99 Å. The ligands adopt an eclipsed orientation (when viewed down the Pd–Pd axis) where both *i*-Pr groups are on the same side of the molecule, with one *i*-Pr substituent directed toward the interior of the dimeric sandwich. The Pd atoms are linked through bridging acetates, giving rise to a Pd1–Pd2 distance of 3.0742(9) Å. The ^1H and ^{13}C NMR spectra of this complex are complex in CD_3CN , likely as a consequence of the diastereotopic isomeric dimers that exist in solution. Complex **5a**, however, has very well-defined NMR spectra, as do all other palladium bis-acetates, **5b–d**.

Single crystals of **6d** were obtained as orange-yellow blocks from an acetonitrile/diethyl ether solution at $-20\text{ }^{\circ}\text{C}$. This dimeric complex crystallizes in the space group $P1$; shown in Figure 6 is the dicationic dimer (two triflate anions also exist in the unit cell but are not within bonding distance to the dimer), which adopts a structure analogous to that of [(neocuproine)-Pd(μ -OAc)] $_2\text{OTf}_2$.³¹ The orientation of the ligand and bridging acetates is such that the pyOx ligands are situated in a partially eclipsed fashion and there is a close contact of 2.9094(4) Å from Pd1 to Pd2. The Pd–N(pyOx) bond distances (1.992(3) and 1.979(3) Å) are shorter than the Pd–N(pyridine) distances (2.096(3) and 2.078(3) Å). The Pd–O distances are all similar. The bond angles about the Pd atoms (excluding the Pd–Pd interaction) reflect a square-planar geometry with angles of 90° . In solution, complex **6d** exhibits a dynamic equilibrium with its monomer, as reported previously for the neocuproine Pd dimers.³¹ At a concentration of approximately

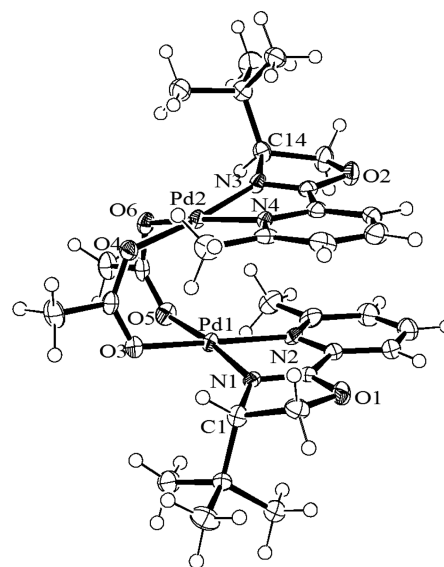
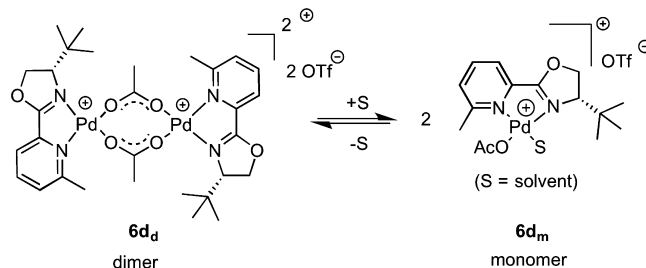


Figure 6. X-ray structure of the bridging acetate dimer **6d**. The two triflate counterions are omitted for clarity. Ellipsoids are drawn at the 50% probability level. Selected bond distances (Å) and bond angles and torsion angles (deg): Pd1–Pd2, 2.9094(4); Pd1–N1, 1.992(3); Pd1–O3, 2.006(3); Pd1–O5, 2.024(3); Pd1–N2, 2.096(3); Pd2–N3, 1.979(3); Pd2–O6, 2.000(3); Pd2–O4, 2.021(3); Pd2–N4, 2.078(3); N1–Pd1–O5, 174.1(2); O3–Pd1–N2, 170.0(1); O6–Pd2–N4, 170.0(1); N1–Pd1–N2, 80.5(1); N3–Pd2–N4, 80.8(1); O6–Pd2–O4, 86.2(1); O3–Pd1–O5, 86.8(1); N1–Pd1–Pd2–N3, 100.1(1); O3–Pd1–Pd2–N3, $-171.49(13)$; O5–Pd1–Pd2–N3, $-83.0(1)$; N2–Pd1–Pd2–N3, 18.4(1); N1–Pd1–Pd2–O6, $-169.1(1)$; O3–Pd1–Pd2–O6, $-80.7(1)$; O5–Pd1–Pd2–O6, 7.8(1); N2–Pd1–Pd2–O6, 109.21(1).

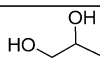
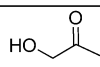
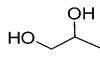
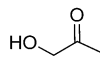
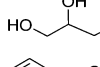
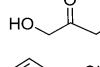
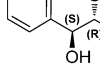
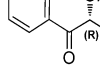
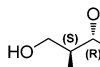
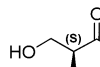
5 mM in in CD_3CN , the complex exists primarily in its monomeric form, [(**L6d**)Pd(OAc)(CD_3CN)]OTf (Scheme 2), as revealed by the concentration-dependent ^1H and ^{13}C NMR spectra.

Scheme 2. Concentration-Dependent Dimer-to-Monomer Equilibration

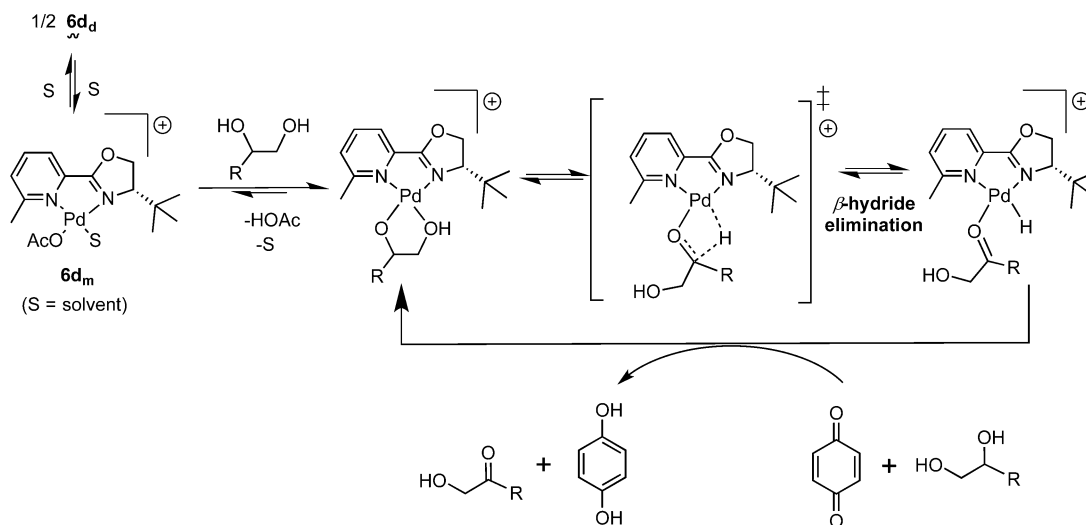


Chemoselective Oxidation of Polyols to Hydroxy Ketones. As our screening experiments had revealed that complex **6d** was both the most active and most chemoselective of the chiral complexes investigated for the oxidation of 1,2-propanediol, we investigated several other alcohols to assess both the chemo- and stereoselectivity. Summarized in Table 1 are results with representative diols, triols, and tetraols. At $60\text{ }^{\circ}\text{C}$, oxidation of 1,2-propanediol with benzoquinone afforded hydroxyacetone with 99% selectivity after 45 min (Table 1, entry 1). Oxidation of glycerol afforded dihydroxyacetone in 87% isolated yield; by ^1H NMR, we could not detect any of the aldehyde resulting from oxidation of the primary alcohol. This

Table 1. Chemo-, Regio-, and Enantioselective Oxidation of Polyols with **6d^f**

Entry	ROH/Pd (mmol)	Substrate	Major Product	t, [T] (h, °C)	Conversion (%) ^a	Yield (%) ^b	ee (%) ^c
1	0.0469/ 0.00468			0.75 [60]	99 ^d	99 ^d	-
2	1.09/ 0.05			24 [55]	95 ^d	87	-
3	1.00/ 0.05			24 [55]	-	85	-
4	1.16/ 0.116			0.91 [55]	99 ^d	71	≤ 11
5	2.05/ 0.204			1.2 [60]	95 ^d	62	24 ^e

^aDetermined by ¹H NMR with *p*-xylene as internal standard. ^bEntry 1 is NMR scale yield with internal standard, entries 2–5 are isolated yields including both enantiomers where applicable. ^cDetermined from HPLC analysis. ^dDetermined by NMR. ^eDetermined from derivatized tris-acetylated compound (see the Experimental Section). ^fAll reactions were performed in 9/1 CH₃CN/H₂O, except for entry 5, where a 2.6/1 ratio was used; deuterated solvents were used for NMR scale reactions. Benzoquinone⁶⁵ was used as a co-oxidant at approximately 1.15 equiv with respect to alcohol.

Scheme 3. Proposed Mechanism for the Oxidation of Diols with Catalyst **6d**

high chemoselectivity for oxidation of the secondary alcohol is analogous to that observed with the achiral [(neocuproine)-Pd(μ -OAc)]₂OTf₂.¹² Oxidation of 1,2,4-butanetriol (entry 3, Table 1) gave 1,4-dihydroxybutanone in 85% yield after 24 h. Oxidation of *meso*-erythritol afforded a 62% isolated yield of erythrulose; NMR experiments reveal that the chemoselectivity in the oxidation of this tetraol is approximately 71% in favor of the α -hydroxy ketone, illustrating the high chemoselectivity of these oxidation reactions for polyols.

Complex **6d** is also efficient at oxidizing mono alcohols such as 2-propanol and 1-propanol to their corresponding ketone or aldehyde. Oxidation of 2-propanol with **6d** (10 mol % Pd) and benzoquinone gave a 56% yield of acetone after 1 h at 65 °C in CD₃CN/D₂O. Under comparable conditions, oxidation of 1-propanol provided a 78% yield of propanal after 1 h, suggesting that the primary alcohol is oxidized faster than the secondary alcohol.³⁹ This was confirmed by oxidation of a 1/1 mixture of 2-propanol and 1-propanol under similar conditions: after 1 h at 65 °C, 1-propanol was oxidized more rapidly than 2-

propanol to give a combined 58% yield of propanal and acetone in a ratio of 1.8. These data indicate that the chemoselectivity for oxidation of primary and secondary alcohols with Pd catalysts derived from **6d** is lower and opposite from that of 1,2-propanediol: 1,2-propanediol is oxidized selectively at the secondary alcohol to afford the hydroxy ketone, whereas mixtures of primary and secondary alcohols exhibit lower selectivities in favor of the primary alcohol.

While the chemoselectivities observed with the chiral complex **6d** are high, the enantioselectivities for the oxidation of *meso*-polyols were modest. Oxidation of *meso*-hydrobenzoin with complex **6d** led to the clean conversion of hydrobenzoin to benzoin with no evidence of the diketone under these conditions (55 °C, approximately 1 h). Analysis of the hydroxy ketone by chiral HPLC revealed the formation of (*R*)-benzoin in 11% ee. To assess if the low enantioselectivities were a consequence of racemization of the resulting hydroxyketones, both (*R,R*)-hydrobenzoin and (*S,S*)-hydrobenzoin were investigated as substrates. NMR scale oxidations of (*R,R*)-hydro-

benzoin or (*S,S*)-hydrobenzoin at 60 °C with **6d** afforded (*R*)-benzoin or (*S*)-benzoin with >90% ee after less than 2 h, implicating that racemization of the hydroxy ketones is minimal under these conditions. Higher enantioselectivities ($\leq 76\%$ ee) were reported for the oxidation of *meso*-hydrobenzoin with $\text{Cu}(\text{OTf})_2$ in the presence of phenyl box ligands of type **L1**.⁶⁶

Oxidation of *meso*-erythritol (entry 5, Table 1) with **6d** cleanly afforded (*S*)-erythrose in 62% isolated yield and 24% ee after column purification. In contrast to *meso*-hydrobenzoin, the *R* alcohol of *meso*-erythritol was oxidized preferentially, albeit with low stereoselectivity.

Proposed in Scheme 3 is a mechanism^{12,31} for the oxidation of vicinal diols by complex **6d**. We propose that complexation of the diol to the monomeric solvate **6d_m** is followed by intramolecular deprotonation⁶⁷ of the coordinated alcohol with loss of HOAc to generate a Pd alkoxide alcohol chelate. β -Hydride elimination would generate the hydroxy ketone adduct of the palladium hydride. Displacement of the hydroxy ketone, subsequent oxidation of the Pd–H by benzoquinone, and substitution by another diol would regenerate the Pd diolate.

The high chemoselectivities exhibited by **6d** for the oxidation of vicinal diols to hydroxy ketones are analogous to those observed for the achiral neocuproine catalysts.¹² On the basis of kinetic and theoretical studies to be reported elsewhere,⁶⁸ we propose that the high chemoselectivity for oxidation of 1,2-propanediol derives from product-determining β -H elimination from the secondary Pd alkoxide to yield the hydroxy ketone. The lower chemoselectivities observed for primary and secondary alcohols is proposed to arise from product-determining equilibration of the Pd alkoxides, favoring the primary alkoxide.

The modest enantioselectivities observed preclude an interpretation of the origin of the enantioselectivity (at 55 °C, an ee of 24% corresponds to a $\Delta\Delta G^\ddagger$ value of <0.5 kcal/mol). If β -H elimination from the solvated diolate **S** (Scheme 3) is the stereodifferentiating step, there are at least two diastereomeric Pd diolates that can form from *meso*-hydrobenzoin, due the lack of C_2 symmetry for ligands **6a–d**. For *meso*-erythritol, the situation is even more complicated, as diolates could form from either the 1,2-position or the 2,2'-position. Crystal structures of neutral Pd diolate complexes of erythritol^{69,70} suggest that the diolate complexes can coordinate at the 1,2-diol position or the 2,2'-position, depending on the coligands. These considerations highlight the challenges for the chemo- and enantioselective oxidation of unprotected polyols. Nevertheless, the high chemoselectivities observed with Pd complexes derived from the chiral ligand **L3d** and the achiral neocuproine,¹² and the impressive enantioselectivities observed with sparteine ligands,^{3,6,15,16} provide promising leads for the further development of alcohol oxidation catalysts capable of both high high chemo- and enantioselectivities.

SUMMARY

Cationic palladium complexes ligated by chiral pyOx ligands are efficient catalysts for the chemoselective oxidation of vicinal polyols to afford α -hydroxy ketones. The activity and selectivity of the Pd catalysts for alcohol oxidation depend sensitively on the ligand environment; complex **6d**, derived from the *tert*-Bu pyOx ligand containing an α -methyl substituent, is more active than pyOx complexes lacking the α -methyl substituent or those derived from bis(oxazoline) or bi(oxazoline) ligands. The oxidation of the vicinal diols 1,2-propanediol and hydrobenzoin, the triol glycerol, and the tetraol erythritol yields the

α -hydroxy ketones with high chemoselectivity in isolated yields of 62–87%. While the chemoselectivities are high, the enantioselectivities observed for the oxidation of *meso*-hydrobenzoin or *meso*-erythritol with the chiral complex **6d** were modest at 11–24% ee.

EXPERIMENTAL SECTION

General Information. All ^1H and $^{13}\text{C}\{^1\text{H}\}$ NMR spectra were obtained at room temperature on Varian 400 MHz, Unity/Inova Varian 500 MHz, or Unity/Inova Varian 600 MHz spectrometers and taken at room temperature. Enantiomeric excess was determined using chiral HPLC (see below for details). For 1,2-propanediol oxidation monitored by ^1H NMR spectra were acquired with $d_1=60$ s, $nt=4$ or 8, $gain=20$ and autoshimmed on a Varian 400 MHz instrument. The chemical shifts are reported in parts per million (δ), and the multiplicities are reported as s (singlet), d (doublet), (triplet), q (quartet), m (multiplet), sept (septet), app (apparent), and br (broad). All peaks were monitored with respect to the *p*-xylene peak (7.00 ppm in $\text{CD}_3\text{CN}/\text{D}_2\text{O}$ solvent mixture and added via microliter syringe). Residual proton and carbon peaks were used as solvent references: ^1H (δ (ppm): chloroform-*d*, 7.26; deuterium oxide-*d*₂, 4.78; acetonitrile-*d*₃, 1.95; dimethyl sulfoxide-*d*₆, 2.49); ^{13}C (δ (ppm): chloroform-*d*, 77.3; acetonitrile, 1.13, 117.1; dimethyl sulfoxide-*d*₆, 39.51). ^{19}F NMR spectra were referenced to the external standard 0.05% α,α,α -CF₃C₆H₅ in C₆D₆ (δ (ppm): C₆D₆; –63.72). LCMS data was obtained from a Waters 2795 HPLC system with a dual-wavelength UV detector and ZQ single quadrupole MS with electrospray ionization (ESI) source and 0.1% formic acid acetonitrile solvent with direct loop injection. High-resolution MS measurements were obtained from an Orbitrap ESI via direct injection or by desorption ESI (DESI; see the Supporting Information). An HP 7890/5975 GC-MS, single quadrupole MS instrument with electron impact ionization source was also used to obtain GC data. Elemental and trace silver analysis was performed at Robertson Microlit Laboratories Inc., Ledgewood, NJ.

X-ray Crystallography. Single crystals were mounted on either a Bruker Kappa X8 or a Bruker D8 Venture diffractometer equipped with an Apex II CCD or Photon 100 CMOS detector, respectively. Frames were collected using ω and ψ scans and integrated with SAINT. Multiscan absorption correction (SADABS) was applied.⁷¹ The structures were solved by direct methods (SHELXS) and refined using full-matrix least squares on F^2 with SHELXL-97⁷² using established procedures.⁷³ Weighted R factors, R_w , and all goodness of fit indicators are based on F^2 . All non-hydrogen atoms were refined anisotropically. The hydrogen atoms of the C–H bonds were placed in idealized positions. Further crystallographic details and the corresponding CIF files can be found in the Supporting Information.

Chemicals. Sodium methoxide (97%), 6-methyl-2-pyridinecarboxitrile (97%), 2-pyridinecarboxitrile (99%), anhydrous toluene (99.8%), glacial acetic acid, *L*-*tert*-leucinol ((*S*)-2-Amino-3,3-dimethyl-1-butanol) (98%), *L*-valinol ((*S*)-2-amino-3-methyl-1-butanol (96%)), (*R*)-(-)-2-phenylglycinol (or (*R*)-2-amino-2-phenylethanol) (98%, 99% ee), (*S,S*)-2,2'-isopropylidene-bis(4-*tert*-butyl-2-oxazoline) (**L1**; 99%), silver acetate (99%), silver trifluoromethanesulfonate ($\geq 99.5\%$), silver tetrafluoroborate (98%), trifluoromethanesulfonic acid (99%), 1,2-propanediol ($\geq 99.5\%$), benzoquinone ($\geq 99.5\%$), *meso*-erythritol (99%), *meso*-hydrobenzoin (99%), (*R,R*)-hydrobenzoin (99%, 99% ee), (*S,S*)-hydrobenzoin (99%, 99% ee), *DL*-benzoin (98%), 1,2,4-butanetriol (98%), and europium(III) trifluoromethanesulfonate (98%) were purchased from Sigma Aldrich. With the exception of benzoquinone (recrystallized in petroleum ether 40–60 °C), all reagents were used as received from Sigma Aldrich. Anhydrous methanol (99.8%) was purchased from Arcos Organics and used as received. Dichloromethane, hexanes, acetonitrile, diethyl ether, ethyl acetate, and ethanol (all ACS grade), *p*-xylene (99.4%), glycerol (99.8%), HPLC grade isopropyl alcohol, and heptane were purchased from Fischer Scientific. *rac*-Erythulose was prepared independently using a previously reported achiral palladium catalyst^{12,68} and *meso*-erythritol and used as the racemic standard for this study.

Dichlorobis(benzonitrile)palladium(II) (99%) and tetrakis(acetonitrile)palladium(II) tetrafluoroborate (99%) were purchased from Strem Chemicals and used as received. CDCl_3 , CD_3CN , and D_2O were obtained from Cambridge Isotopes Laboratories and used as received.

Ligand Synthesis. Ligand **L1**, (*S,S*)-2,2'-isopropylidene-bis(4-*tert*-butyl-2-oxazoline), was purchased from Sigma-Aldrich and used as received.

Bi(oxazoline) ligands **L2a,b** were prepared by literature methods⁴⁶ and characterized by ^1H NMR and GC-MS (see the Supporting Information).

Ligands **L3a–d** were prepared according to Scheme 1 from 2-pyridinecarbonitrile or 6-methylpicolinonitrile. A detailed procedure is given below for **L3d**; ligands **L3a–c** were prepared following a similar procedure⁵⁶ (see the Supporting Information). Compounds **2a,b** were synthesized according to the literature.⁴²

Synthesis of 2b.⁴² NaOMe (4.15 g, 0.0768 mol) was placed in a 50 mL pear-shaped round-bottomed flask in a nitrogen glovebox. Under a stream of argon, anhydrous MeOH (18 mL) was added and stirred, dissolving the NaOMe. During this time the solution became warm. 6-Methyl-2-pyridinecarbonitrile (**1**; 4.0 g, 0.0338 mol) was dissolved in 20 mL of anhydrous toluene. The toluene solution was added to the stirred MeOH solution and left to react for at least 4 h at room temperature. HOAc (4.61 g, 0.0767 mol) was added to the solution, during which the solution became gelatinous. The solution was then dried under vacuum to reveal a white powder in an oily liquid. The residue was then dissolved in 25 mL of dichloromethane and the insoluble residue was filtered by gravity. The brown solution was dried under vacuum to reveal a brown oil. The brown oil was vacuum-distilled at 60 °C at 60 mTorr to give a colorless oil and used the same day. Yield: 4.1 g (81%). ^1H NMR (CDCl_3 , 400 MHz): 7.58–7.68 (m, 2H), 7.18 (ddd, $J = 6.87, 0.41$ Hz, 1H), 3.97 (s, 3H), 2.55 (s, 3H). ^{13}C NMR (125 MHz, CDCl_3): 167.34, 158.45, 146.99, 137.57, 125.31, 118.23, 54.08, 24.69. GC-MS (EI): calculated for $\text{C}_8\text{H}_{10}\text{N}_2\text{O}$ 150.08, found m/z (EI) M^+ 150.1.

Synthesis of (S)-4-(*tert*-Butyl)-2-(6-methylpyridin-2-yl)-4,5-dihydrooxazole (L3d). Compound **2b** (4.12 g, 0.0274 mol) was placed in a 50 mL round-bottomed flask. *L-tert*-Leucinol ((*S*)-2-amino-3,3-dimethyl-1-butanol; 3.22 g, 0.0274 mol) was added. The flask was heated to 65 °C and the mixture stirred under a gentle stream of argon (to aid in evaporation of volatiles) for 16 h. During this time, the slightly greenish solution solidified. The reaction mixture was cooled to room temperature, and the residue was recrystallized from petroleum ether (36–60 °C) and dried under vacuum to reveal a white, needlelike powder. Yield: 5.05 g (84%). Alternatively, the ligand can be purified by flash silica gel chromatography, with 5/1 hexanes/ethyl acetate as eluent. ^1H NMR (CDCl_3 , 400 MHz): 7.94 (d, $J = 7.60$ Hz, 1H), 7.65 (t, $J = 7.74$ Hz, 1H), 7.24 (d, $J = 7.17$ Hz, 1H, overlapping with residual solvent peak), 4.45 (dd, $J = 10.18$ Hz, 1H), 4.31 (t, $J = 8.50$ Hz, 1H), 4.10 (dd, $J = 10.24$ Hz, 1H), 2.63 (s, 3H), 0.96 (s, 9H). ^{13}C NMR (125 MHz, CDCl_3): 162.86, 158.82, 146.66, 136.90, 125.46, 121.50, 76.56, 69.58, 34.23, 26.17, 24.92. GC-MS (EI): calculated for $\text{C}_{13}\text{H}_{18}\text{N}_2\text{O}$ 218.14, found m/z (EI) M^+ 218.1.

Pd Complexes. Screening of palladium complexes with ligands **L1** and **L2** and their syntheses are described in the Supporting Information. The syntheses of compounds **4d–6d** are described in detail below; complexes **4a–c**, **5a–c**, and **6a–c** were prepared analogously (see the Supporting Information).

Synthesis of Dichloropalladium (S)-4-(*tert*-Butyl)-2-(6-methylpyridin-2-yl)-4,5-dihydrooxazole-6-methylpicolinonitrile (4d). Compound **L3d** (4.25 g, 0.0194 mol) was placed in a 200 mL round-bottomed flask equipped with a stir bar. $(\text{PhCN})_2\text{PdCl}_2$ (7.305g, 0.01904 mmol) was added to the flask. A 50 mL portion of dichloromethane was added, and a deep red solution formed. The solution was stirred for 18 h at room temperature. The volume was reduced to one-fourth of the original solvent under vacuum. Hexanes was added to precipitate out an orange-brown product. The supernatant was carefully decanted, and the precipitate was washed and triturated with 3 × 100 mL of hexanes or until the supernatant became clear. The precipitate was dried under vacuum (60 mTorr)

with 50 °C heating. Yield: 7.89 g, 92% (with a half-molecule of dichloromethane in molecular weight). Attempts to remove the solvate with prolonged heating (50–90 °C) under vacuum or redissolving in other solvents (MeCN, ether) led to decomposition or new solvent incorporation, respectively. ^1H NMR (300 MHz, CDCl_3): 7.96 (t, $J = 7.76$ Hz, 1H), 7.67 (dd, $J = 7.51$ Hz, 1H), 7.53 (dd, $J = 8.01$ Hz, 1H), 5.28 (s, 1H, $1/2$ dichloromethane), 4.86 (dd, $J = 9.32$ Hz, 1H), 4.74 (t, $J = 9.27$ Hz, 1H), 4.41 (dd, $J = 9.18$ Hz, 1H), 3.14 (s, 3H), 1.05 (s, 9H). ^{13}C NMR (125 MHz, CDCl_3): 169.07, 167.86, 144.70, 139.54, 131.72, 123.01, 73.97, 69.54, 53.7 (DCM), 35.46, 27.61, 26.04. Anal. Calcd for $[(\text{L3d})\text{PdCl}_2] \cdot 1/2 \text{CH}_2\text{Cl}_2$ ($\text{C}_{13}\text{H}_{18}\text{Cl}_2\text{N}_2\text{O} \cdot 1/2 \text{CH}_2\text{Cl}_2$): C, 38.18; H, 4.47; N, 6.72. Found: C, 38.31; H, 4.21; N, 6.63. MS (ESI): m/z found 400.1 (calcd for $[(\text{L3d})\text{Pd}(\text{MeCN})\text{Cl}]^+ 400.04$). X-ray-quality crystals were grown by slow evaporation of a dichloromethane solution at room temperature, to reveal large red crystals (see Figure 4 and the Supporting Information).

Synthesis of Diacetatopalladium (S)-4-(*tert*-Butyl)-2-(6-methylpyridin-2-yl)-4,5-dihydrooxazole-6-methylpicolinonitrile (5d). Compound **4d** (7.33 g, 0.0176 mol, with $1/2$ MeCN solvate as dry weight determined by ^1H NMR, solvent corrected mol wt of 416.14 g/mol) was placed in a 250 mL round-bottomed flask equipped with a stir bar and wrapped in aluminum foil. AgOAc (6.28 g, 0.0376 mol) was added to the flask under a stream of argon. A 50 mL portion of dichloromethane was added, and the mixture was stirred in the dark for 45 min. Under a stream of argon, the solution was filtered through a plug of Celite and evaporated to dryness for several hours to reveal an orange precipitate. Yield: 8.48 g (89% with $1/2$ dichloromethane as judged by ^1H NMR). The precipitate was used immediately for the next step. ^1H NMR (300 MHz, CDCl_3): 7.96 (t, $J = 7.47$ Hz, 1H), 7.57 (d, $J = 7.44$ Hz, 1H), 7.43 (d, $J = 7.47$ Hz, 1H), 4.90–4.51 (m, 2H), 3.87 (dd, $J = 8.54$ Hz, 1H), 2.66 (s, 3H), 2.00 (s, 3H), 1.96 (s, 3H), 0.97 (s, 9H). ^{13}C NMR (125 MHz, CDCl_3): 178.75, 178.356, 169.966, 166.354, 144.822, 139.719, 131.462, 122.822, 73.602, 72.209, 34.860, 25.930, 23.961, 23.086, 23.018 (br sh). MS (ESI): m/z found $[\text{M} - \text{OAc}]^+ 383.1$ (100%) (calcd 383.06, 100%).

Synthesis of [(pyOx)Pd(OAc)]₂[OTf]₂ (6d). A 0.33 M HOTf solution was prepared freshly from anhydrous acetonitrile. A 53 mL portion (0.0179 mol) of this solution was added directly to a powder containing compound **5d** (8.48 g, 0.0174 mol, with $1/2$ dichloromethane solvate as dry weight determined by ^1H NMR, solvent corrected mol wt of 485.26 g/mol), and the mixture was stirred for 45 min. A deep red solution formed. A 650 mL portion of anhydrous diethyl ether was added to the solution, and an orange precipitate formed. The solution was placed in a –20 °C freezer for 1 h. The supernatant was carefully decanted, and the residue was washed with 3 × 100 mL of ether or until the washings became clear. The orange precipitate was dried overnight under vacuum at 40 °C to give 7.20 g of orange product. Another 0.61 g was recovered from the washing solutions following the same procedure as above. Overall yield: 7.80 g, 86% (78% from $(\text{PhCN})_2\text{PdCl}_2$). ^1H NMR of $[(\text{pyOx})\text{Pd}(\text{OAc})\text{-(CH}_3\text{CN)}][\text{OTf}]$ (**6d_m**) (600 MHz, CD_3CN , 4.8 mM solution, approximately 5% dimer present): 8.13 (t, $J = 7.82$ Hz, 1H), 7.74 (dd, $J = 7.59$ Hz, 1H), 7.67 (d, $J = 7.89$ Hz, 1H), 4.99 (dd, $J = 9.66$ Hz, 1H), 4.82 (t, $J = 9.53$ Hz, 1H), 3.88 (v br, 1H), 2.69 (s, 3H), 1.93 (br s, 3H), 1.00 (s, 9H). ^1H NMR of $[(\text{pyOx})\text{Pd}(\text{OAc})_2][\text{OTf}]_2$ (**6d_d**) (600 MHz, CD_3CN , 448 mM solution, approximately 35% **6d_m**): 8.29 (t, $J = 7.81$ Hz, 1H), 7.89 (d, $J = 7.90$ Hz, 1H), 7.68 (d, $J = 7.44$ Hz, 1H, overlapping with **6d_m**), 4.80 (dd, $J = 10.42$ Hz, 1H, overlapping with **6d_m**), 4.04 (t, $J = 9.89$ Hz, 1H), 3.51 (dd, $J = 9.29$ Hz, 1H), 2.72 (s, 3H), 2.17 (s, 3H), 0.99 (s, 9H, overlapping with **6d_m**). ^{13}C NMR of $[(\text{pyOx})\text{Pd}(\text{OAc})_2][\text{OTf}]_2$ (**6d_d**) (125 MHz, CD_3CN , 448 mM solution): 188.151, 170.386, 167.385, 142.909, 133.812, 126.752, 74.370, 71.010, 35.550, 24.906, 24.563, 24.068, 23.272. CF_3SO_3^- not observed. ^{19}F NMR (376 MHz, CD_3CN): –80.41. HR-MS ESI Orbitrap (neat CD_3CN): found m/z (relative intensity) 383.0581 (100%) $[\text{O}5\text{M} - \text{CF}_3\text{SO}_3^-]$ (calcd 383.0582 (100%) agrees within 0.2 ppm for $\text{C}_{15}\text{H}_{21}\text{N}_2\text{O}_3\text{Pd}^+$, i.e. Pd monomer (singly cationic) species) complete isotope pattern 383.0581 (100%), 385.0579 (88.78%), 382.0596 (80.00%), 387.0590 (38.64%), 381.0584 (35.69%), 384.0610 (13.90%), 386.0611 (13.32%), 388.0621 (5.40%), 379.0600 (2.61%).

Anal. Calcd for [(L3d)Pd(OAc)][OTf] (C₁₆H₂₁F₃N₂O₆PdS): C, 36.07; H, 3.97; N, 5.26. Found: C, 35.82; H, 3.71; N, 5.15. X-ray-quality single crystals were grown from diethyl ether diffusion into a concentrated acetonitrile solution at approximately -20 °C (see Figure 6 and the Supporting Information). We also performed ICP trace metal analysis for silver and obtained 2650 ppm (0.26%) of silver in this sample. This sample was used for all preparatory scale oxidation catalyses described in this paper. Control experiments reveal that Ag(L3d)⁺ is inactive for alcohol oxidation (see the Supporting Information).

Alcohol Oxidation: Screening Experiments. A series of screening experiments (NMR and preparatory scale) were conducted in order to determine which ligand set had the most promising activity for 1,2-propanediol oxidation (NMR scale). Screening experiments were done on systems containing ligands L1, L2a, L2b, and L3a–L3d, where the latter was found to be superior and studied in detail.

Oxidation of 1,2-Propanediol with [(L2b)Pd(MeCN)₂][BF₄]₂/C₅H₅CO₂. [(L2b)Pd(MeCN)₂][BF₄]₂ (5 mg, 0.00813 mmol) was added to a 0.7 mL DMSO-*d*₆ solution containing 1,2-propanediol (6.2 mg, 5.9 μL, 0.0815 mmol), C₅H₅CO₂ (1.3 mg, 0.00398 mmol), benzoquinone (17.6 mg, 0.162 mmol), and *p*-xylene (8.6 mg, 10 μL, 0.081 mmol). At room temperature, less than 7% conversion was observed over the course of 2 days; however, heating the same solution to 60 °C for 1 h led to a 23% yield of hydroxyacetone, as determined by integration vs the internal standard *p*-xylene (with relaxed ¹H NMR spectra, 400 MHz) with significant Pd black formation. Other attempts to generate the active catalyst in situ involved addition of HOTf to the palladium bis-acetate complexes;³² addition of 1 equiv of HOTf (29 μL, 0.33 M HOTf in a MeCN solution) to a 0.7 mL CD₃CN stock solution containing (L2a)PdOAc₂ (4.3 mg, 0.01 mmol), benzoquinone (21.6 mg, 0.200 mmol), and 1,2-propanediol (7.5 mg, 0.100 mmol) revealed no evidence of hydroxyacetone formation after 18 h at room temperature.

NMR Scale Oxidation Reactions. Oxidation of 1,2-Propanediol. 1,2-Propanediol (3.57 mg, 0.0469 mmol), benzoquinone (5.6 mg, 0.0518 mmol), and *p*-xylene (5.5 mg, 0.0519 mmol) was dissolved in 0.7 mL of a 8/1 CD₃CN/D₂O solution. To this solution was added 2.5 mg of 6d (0.00468 mmol), and the NMR tube was placed in a heated oil bath at 60 °C. After 45 min, another ¹H NMR measurement was taken to reveal the formation of hydroxyacetone. ¹H NMR (9/1 CD₃CN/D₂O, 400 MHz): 4.12 (s, 2H), 2.04 (s, 3H). See the Supporting Information for ¹H NMR.

Preparative Scale Oxidation Reactions. Oxidation of Glycerol. Glycerol (100 mg, 1.09 mmol) and benzoquinone (130 mg, 1.2 mmol) were dissolved in 10 mL of a 9/1 acetonitrile/water mixture. Catalyst 6d (26.6 mg, 0.05 mmol) was added, and over a few minutes, the reaction mixture darkened. The mixture was stirred for 24 h at 55 °C. Upon completion of the reaction, a palladium mirror was observed on the walls of the vial. After completion, the mixture was rotary evaporated at 40 °C. This mixture was rotary evaporated, and the residue was dissolved in 15/1 ethyl acetate/ethanol and then purified through silica gel chromatography, using a gradient elution of neat ethyl acetate to 7/1 ethyl acetate/ethanol. Evaporation of the relevant fractions gave 85 mg (0.944 mmol, 87% yield) of off-white flakes. In D₂O, dihydroxyacetone exists in equilibrium between the free and hydrated forms. ¹H NMR (500 MHz, D₂O): 4.34 (s, 1 H) (free). ¹³C NMR (126 MHz, D₂O): 65.48, 212.61 (free). ¹H NMR (500 MHz, D₂O): ppm 3.50 (s, 1 H) (hydrated). ¹³C NMR (126 MHz, D₂O): 64.17, 95.71 (hydrated). See the Supporting Information.

Oxidation of 1,2,4-Butanetriol. 1,2,4-Butanetriol (106 mg, 1 mmol) and benzoquinone (130 mg, 1.2 mmol) were dissolved in 10 mL of a 9/1 acetonitrile/water mixture. Catalyst 6d (26.6 mg, 0.05 mmol) was added, and over a few minutes, the reaction mixture darkened. The mixture was stirred for 24 h at 55 °C. The reaction progress was monitored via TLC, using 20/1 ethyl acetate/ethanol as the eluent. After completion of the reaction, the mixture was rotary evaporated at 40 °C. The residue was dissolved in a 2 mL portion of acetonitrile and then twice purified through silica gel chromatography. The first time 20/1 ethyl acetate/ethanol was used as an eluent, and the second time a gradient elution of neat ethyl acetate to 15/1 ethyl acetate/ethanol

was performed. Evaporation of the relevant fractions gave 88 mg (0.85 mmol, 85% yield) of a light brownish oil. ¹H NMR (500 MHz, D₂O): 2.63 (t, *J* = 5.86 Hz, 2 H) 3.78 (t, *J* = 5.86 Hz, 2 H) 4.30 (s, 2 H). ¹³C NMR (126 MHz, D₂O): 40.92 (s, 1 C) 57.02 (s, 1 C) 68.30 (s, 1 C) 212.82 (s, 1 C).

Oxidation of meso-Hydrobenzoin. meso-Hydrobenzoin (250 mg, 1.16 mmol) and recrystallized benzoquinone (150 mg, 1.37 mmol) were dissolved in 18.0 mL of a 9/1 CH₃CN/H₂O mixture in a 200 mL pear-shaped round-bottomed flask. The solution was stirred until the reactants dissolved. Pd catalyst 6d (62.1 mg, 0.116 mmol using monomer molecular weight of 532.01 g/mol) was added to the vial. The flask was capped and placed in a 55 °C oil bath and the reaction monitored by ¹H NMR spectroscopy. Previous NMR experiments revealed a maximum yield of 100% for this reaction under the same conditions. After 1.2 h, the solution was evaporated to dryness with 35 °C heating to reveal a dark black-green mixture. The crude product was dissolved in a minimum amount of EtOAc solution and triturated with slight heating and sonication and then loaded onto a column using 15/1 hexanes/EtOAc eluent. The silica column had dimensions of 18 cm × 2.5 cm in a 35 cm length column. The product has an *R_f* value of 0.3 and comes out immediately after the BQ-HQ fraction. Some coelution is observed with the BQ-HQ fractions, which is responsible for lower isolated yields. The product-containing fractions were combined and evaporated to dryness to reveal a white precipitate in 71% yield (176 mg). ¹H NMR (500 MHz, CDCl₃): 7.94 (dd, *J* = 8.44 Hz, 2H), 7.55 (t, *J* = 7.44 Hz, 1H), 7.42 (t, *J* = 7.77 Hz, 2H), 7.39–7.27 (m, 5H), 5.98 (d, *J* = 6.10 Hz, 1H), 4.59 (d, *J* = 6.09 Hz, 1H). ¹³C NMR (125 MHz, CDCl₃): 199.168, 139.229, 134.195, 133.671, 129.410, 129.400 (sh), 128.952, 128.850, 128.027, 76.460. GC-MS (EI): *m/z* 212. Chiral HPLC was carried out by a modified literature preparation:⁶⁶ Chiralcel OJ-H, iPrOH/heptane 10/90, flow rate of 0.8 mL/min and 210 nm detection with manual injection; (*R*)-benzoin, 18.9 min; (*S*)-benzoin, 22.8 min; 5–11% ee was observed over multiple runs in favor of the *R* enantiomer (major). The sample was compared to the commercial DL-benzoin.

Oxidation of meso-Erythritol. meso-Erythritol (250 mg, 2.05 mmol) and recrystallized benzoquinone (234 mg, 2.16 mmol) were dissolved in a 30.0 mL solution of a 2.6/1 CH₃CN/H₂O mixture in a 200 mL pear-shaped round-bottom flask. The solution was stirred until the reactants dissolved. Pd catalyst 6d (108.9 mg, 0.204 mmol) was added to the flask. The solution was sealed and placed in a 60 °C heated oil bath, and the conversion was monitored by ¹H NMR spectroscopy. After 1.2 h, the solution was evaporated to dryness at 35 °C to reveal a dark black-green syrupy mixture. The crude product was dissolved in a minimal amount of a 20/1 EtOAc/EtOH mixture, triturated, heated slightly, and sonicated. The crude mixture was loaded onto a silica column (18 cm × 2.5 cm in a 35 cm length column) and eluted with a 20/1 EtOAc/EtOH mixture. The product has an *R_f* value of 0.4 and comes out soon after the BQ-HQ fraction. The product-containing fractions were combined and evaporated to dryness to reveal a syrupy colorless oil in 61% yield (140 mg). Previous NMR experiments reveal a maximum yield of 71% for this reaction under the same conditions. ¹H NMR (400 MHz, D₂O): 4.61–4.44 (m, 2H), 4.42 (t, *J* = 4.08 Hz, 1H), 3.83 (q, *J* = -1.5 Hz, 2H). ¹³C NMR (125 MHz, D₂O with MeOH internal standard, 49.13 ppm): 212.546, 76.149, 66.107, 63.138.

Derivatization of Erythrose to Erythrose Triacetate for Chiral HPLC Analysis. This procedure was performed by a modified literature procedure.⁷⁴ When Eu(OTf)₃ was used rather than Er(OTf)₃, we found that the isolated yields doubled. Erythrose (137 mg, 1.14 mmol) and Eu(OTf)₃ (8.0 mg, 0.0135 mmol) was placed in a 100 mL pear-shaped round-bottomed flask equipped with a stir bar. The flask was filled with argon. Simultaneously, 7 mL of anhydrous MeCN and Ac₂O (0.40 mL, 0.432 g, 4.23 mmol) were added to a septum-sealed flask with dynamic argon. The solution was stirred at room temperature for 17 h under static argon. After approximately 2 h of stirring, all of the erythrose had completely dissolved to give a slightly green solution. The reaction was monitored by ¹H NMR for completion. After 17 h, 40 mL of ethyl acetate was added to the mixture and it was extracted with a 50 mL saturated

NaHCO₃ solution. The organic phase was dried under vacuum and purified by flash silica chromatography using 1/1 EtOAc/hexanes as eluent to give a colorless oil with a slight green tinge to it. The product had an *R_f* factor of approximately 0.6. Yield: 236 mg (62%). ¹H NMR (400 MHz, CDCl₃): 5.40 (dd, *J* = 5.00 Hz, 1H), 4.91–4.80 (dd, 2H), 4.50 (dd, *J* = 12.26 Hz, 1H), 4.38 (dd, *J* = 12.26 Hz, 1H), 2.18 (s, 3H), 2.17 (s, 3H), 2.08 (s, 3H). ¹³C NMR (100 MHz, CDCl₃): 198.621, 170.602, 170.216, 170.041, 74.902, 66.866, 62.586, 20.842, 20.750, 20.591. Chiral HPLC analysis: Chiralcel AD-H, iPrOH/heptane 5/95, flow rate 0.8 mL/min and 210 nm detection with manual injection; (R)-erythrose trisacetate, 22.0 min; (S)-erythrose trisacetate, 25.4 min; 24% ee was observed (38% (R)-erythrose trisacetate, 62% (S)-erythrose trisacetate). The sample was compared with rac-erythrose trisacetate synthesized in our laboratory (see Chemicals above).

DFT Computations. Computations were performed using the Gaussian 09⁷⁵ software package in a Linux multiprocessor environment. Geometry optimizations and vibration analysis were performed using the M06-L DFT functional as described by Truhlar and Zhao⁷⁶ with the double- ζ polarized 6-31G(d,p)^{77–86} basis set for light atoms and SDD⁸⁷ ecp for Pd and added *f* coefficients^{88–90} and default convergence criteria in the gas phase. All calculations were performed with the a cationic charge and singlet ground state multiplicities in the gas phase. The GEDIIS algorithm was used for geometry optimizations. All stationary point structures were confirmed to be local minima as determined by vibration analysis, where no imaginary or negative frequencies were present for the intermediates. SCF energies are not ZPE corrected. See the Supporting Information for atomic coordinates and SCF energies.

■ ASSOCIATED CONTENT

■ Supporting Information

Text, figures, tables, and CIF files giving NMR spectra, GC and LS-MS data, chiral HPLC traces, X-ray crystallography data, and DFT computed atomic coordinates. This material is available free of charge via the Internet at <http://pubs.acs.org>. The crystal structures have been deposited at the Cambridge Crystallographic Data Centre (CCDC) and allocated with the deposition numbers CCDC 928778–928781.

■ AUTHOR INFORMATION

■ Corresponding Author

*E-mail for R.M.W.: waymouth@stanford.edu.

■ Notes

The authors declare no competing financial interest.

■ ACKNOWLEDGMENTS

This research was supported by Department of Energy (DE-FG02-10ER16198). A.G.D.C. acknowledges Stanford University for a Center for Molecular Analysis and Design (CMAD) postdoctoral fellowship. K.C. is grateful for a Stanford Graduate Fellowship. We thank Autumn Maruniak in the Trost Laboratory for assistance with chiral HPLC. We thank Dr. Stephen R. Lynch for assistance with NMR measurements, Dr. Richard Perry for Orbitrap HRMS of complex **6d** and Andrew Ingram for **4c** and the CH-activated Pd complex of **L1**. We thank GCEP, Professor T. Daniel P. Stack, and Eric Stenehjem for access and maintenance of the Redox computer cluster (Stanford University) to perform the DFT computations.

■ REFERENCES

- (1) Arterburn, J. B. *Tetrahedron* **2001**, *57*, 9765–9788.
- (2) Sheldon, R. A.; Arends, I. W. C. E.; ten Brink, G.-J.; Dijkman, A. *Acc. Chem. Res.* **2002**, *35*, 774–781.
- (3) Schultz, M. J.; Sigman, M. S. *Tetrahedron* **2006**, *62*, 8227–8241.
- (4) Parmeggiani, C.; Cardona, F. *Green Chem.* **2012**, *14*, 547–564.
- (5) Muzart, J. *Tetrahedron* **2003**, *59*, 5789–5816.
- (6) Gligorich, K. M.; Sigman, M. S. *Chem. Commun.* **2009**, 3854–3867.
- (7) Arends, I. W. C. E.; Sheldon, R. A. In *Modern Oxidation Methods*; Wiley-VCH: Weinheim, Germany, 2005; pp 83–118.
- (8) Marko, I. E.; Giles, P. R.; Tsukazaki, M.; Chelle-Regnaut, I.; Gautier, A.; Dumeunier, R.; Philippart, F.; Doda, K.; Mutonkole, J.-L.; Brown, S. M.; Urch, C. J. In *Advances in Inorganic Chemistry*; van Eldik, R., Ed.; Academic Press: New York, 2004; Vol. 56, pp 211–240.
- (9) Hoover, J. M.; Stahl, S. S. *J. Am. Chem. Soc.* **2011**, *133*, 16901–16910.
- (10) Mallat, T.; Baiker, A. *Chem. Rev.* **2004**, *104*, 3037–3058.
- (11) Zhan, B. Z.; Thompson, A. *Tetrahedron* **2004**, *60*, 2917–2935.
- (12) Painter, R. M.; Pearson, D. M.; Waymouth, R. M. *Angew. Chem., Int. Ed.* **2010**, *49*, 9456–9459.
- (13) Bettucci, L.; Bianchini, C.; Filippi, J.; Lavacchi, A.; Oberhauser, W. *Eur. J. Inorg. Chem.* **2011**, 1797–1805.
- (14) Noronha, G.; Henry, P. M. *J. Mol. Catal. A: Chem.* **1997**, *120*, 75–87.
- (15) Ebner, D.; Trend, R.; Genet, C.; Mcgrath, M.; O'Brien, P.; Stoltz, B. *Angew. Chem., Int. Ed.* **2008**, *47*, 6367–6370.
- (16) Ebner, D. C.; Bagdanoff, J. T.; Ferreira, E. M.; McFadden, R. M.; Caspi, D. D.; Trend, R. M.; Stoltz, B. M. *Chem. Eur. J.* **2009**, *15*, 12978–12992.
- (17) Mandal, S. K.; Jensen, D. R.; Pugsley, J. S.; Sigman, M. S. *J. Org. Chem.* **2003**, *68*, 4600–4603.
- (18) Arends, I. W. C. E.; ten Brink, G.-J.; Sheldon, R. A. *J. Mol. Catal. A: Chem.* **2006**, *251*, 246–254.
- (19) Steinhoff, B. A.; Stahl, S. S. *J. Am. Chem. Soc.* **2006**, *128*, 4348.
- (20) Nishimura, T.; Onoue, T.; Ohe, T.; Uemura, S. *J. Org. Chem.* **1999**, *64*, 6750–6755.
- (21) Iwasawa, T.; Tokunaga, M.; Obora, Y.; Tsuji, Y. *J. Am. Chem. Soc.* **2004**, *126*, 6554–6555.
- (22) ten Brink, G.-J.; Arends, I. W. C. E.; Sheldon, R. A. *Science* **2000**, *287*, 1636–1639.
- (23) Schultz, M. J.; Park, C. C.; Sigman, M. S. *Chem. Commun.* **2002**, 3034–3035.
- (24) Jensen, D. R.; Schultz, M. J.; Mueller, J. A.; Sigman, M. S. *Angew. Chem., Int. Ed.* **2003**, *42*, 3810–3813.
- (25) Nishimura, T.; Onoue, T.; Ohe, K.; Uemura, S. *Tetrahedron Lett.* **1998**, *39*, 6011–6014.
- (26) Ferreira, E. M.; Stoltz, B. M. *J. Am. Chem. Soc.* **2001**, *123*, 7725–7726.
- (27) Trend, R. M.; Stoltz, B. M. *J. Am. Chem. Soc.* **2008**, *130*, 15957–15966.
- (28) Jensen, D. R.; Pugsley, J. S.; Sigman, M. S. *J. Am. Chem. Soc.* **2001**, *123*, 7475–7476.
- (29) Melero, C.; Shishilov, O. N.; Alvarez, E.; Palma, P.; Campora, J. *Dalton Trans.* **2012**, *41*, 14087–14100.
- (30) Bailie, D. S.; Clendenning, G. M. A.; McNamee, L.; Muldoon, M. J. *Chem. Commun.* **2010**, *46*, 7238–7240.
- (31) Conley, N. R.; Labios, L. A.; Pearson, D. M.; McCrory, C.; Waymouth, R. M. *Organometallics* **2007**, *26*, 5447–5453.
- (32) Pearson, D. M.; Conley, N. R.; Waymouth, R. M. *Organometallics* **2011**, *30*, 1445–1453.
- (33) Pearson, D. M.; Waymouth, R. M. *Organometallics* **2009**, *28*, 3896–3900.
- (34) Hoyos, P.; Sinisterra, J. V.; Molinari, F.; Alcantara, A. R.; De Maria, P. D. *Acc. Chem. Res.* **2010**, *43*, 288–299.
- (35) Hanessian, S.; Roy, R. *J. Am. Chem. Soc.* **1979**, *101*, 5839–5841.
- (36) Trost, B. M.; Ito, H.; Silcoff, E. R. *J. Am. Chem. Soc.* **2001**, *123*, 3367–3368.
- (37) Davis, F. A.; Chen, B. C. *Chem. Rev.* **1992**, *92*, 919–934.
- (38) ten Brink, G.-J.; Arends, I. W. C. E.; Hoogenraad, M.; Verspui, G.; Sheldon, R. A. *Adv. Synth. Catal.* **2003**, *345*, 1341–1352.
- (39) ten Brink, G.-J.; Arends, I. W. C. E.; Sheldon, R. A. *Adv. Synth. Catal.* **2002**, *344*, 355–369.
- (40) Desimoni, G.; Faita, G.; Jørgensen, K. A. *Chem. Rev.* **2006**, *106*, 3561–3651.

- (41) McManus, H. A.; Guiry, P. J. *Chem. Rev.* **2004**, *104*, 4151.
- (42) Oila, M. Ph.D. Thesis, Doctor of Science in Technology, Helsinki University of Technology, 2008; p 54.
- (43) Rasappan, R.; Laventine, D.; Reiser, O. *Coord. Chem. Rev.* **2008**, *252*, 702–714.
- (44) He, W.; Yip, K.-T.; Zhu, N.-Y.; Yang, D. *Org. Lett.* **2009**, *11*, 5626–5628.
- (45) Jiang, F.; Wu, Z.; Zhang, W. *Tetrahedron Lett.* **2012**, *51*, 5124–5126.
- (46) Denmark, S. E.; Stavenger, R. A.; Faucher, A.-M.; Edwards, J. P. *J. Org. Chem.* **1997**, *62*, 3375–3389.
- (47) Ebinger, A.; Heinz, T.; Umbricht, G.; Pfaltz, A. *Tetrahedron* **1998**, *54*, 10469.
- (48) Bouch, R.; Scheurer, A.; Mosset, P.; Saalfrank, R. W. *Tetrahedron Lett.* **2000**, *41*, 1023.
- (49) Brunner, H.; Obermann, U.; Wimmer, P. *J. Organomet. Chem.* **1986**, *316*, C1–C3.
- (50) Chelucci, G.; Medici, S.; Saba, A. *Tetrahedron: Asymmetry* **1997**, *8*, 3183–3184.
- (51) Chelucci, G.; Medici, S.; Saba, A. *Tetrahedron: Asymmetry* **1999**, *10*, 543–550.
- (52) Yoo, K. S.; Park, C. P.; Yoon, C. H.; Sakaguchi, S.; O'Neill, J.; Jung, K. W. *Org. Lett.* **2007**, *9*, 3933–3935.
- (53) Jana, R.; Pathak, T. P.; Jensen, K. H.; Sigman, M. S. *Org. Lett.* **2012**, *14*, 4074–4077.
- (54) Yang, G.; Shen, C.; Zhang, W. *Angew. Chem., Int. Ed.* **2012**, *51*, 9141–9145.
- (55) Kikushima, K.; Holder, J. C.; Gatti, M.; Stoltz, B. M. *J. Am. Chem. Soc.* **2011**, *133*, 6902–6905.
- (56) Brunner, H.; Obermann, U. *Chem. Ber.* **1989**, *122*, 499.
- (57) Bolm, C.; Weickhardt, K.; Zehnder, M.; Ranff, T. *Chem. Ber.* **1991**, *124*, 1173–1180.
- (58) Podhajsky, S. M.; Iwai, Y.; Cook-Sneathen, A.; Sigman, M. S. *Tetrahedron* **2011**, *67*, 4435–4441.
- (59) Keuseman, K. J.; Smoliakova, I. P.; Dunina, V. V. *Organometallics* **2005**, *24*, 4159–4169.
- (60) Zehnder, M.; Neuburger, M. *Acta Crystallogr.* **1995**, *C51*, 1109–1112.
- (61) Jones, M. D.; Almeida Paz, F. A.; Davies, J. E.; Raja, R.; Duer, M.; Klinowski, J.; Johnson, B. F. G. *Inorg. Chim. Acta* **2004**, *357*, 3351–3359.
- (62) Kožiček, J.; Fronc, M.; Svoboda, I.; Kapitaňan, P.; Gracza, T. *Acta Crystallogr.* **2004**, *E60*, m1895–m1896.
- (63) Shen, W.-Z.; Gupta, D.; Lippert, B. *Inorg. Chem.* **2005**, *44*, 8249–8258.
- (64) Kazi, A. B.; Jones, G. C.; Vicic, D. A. *Organometallics* **2005**, *24*, 6051–6054.
- (65) Complex **6d** is also active for aerobic oxidation of polyols. For oxidations in air, conversions and yields are lower, but the enantioselectivity for the oxidation of *meso*-erythritol is similar to that observed with benzoquinone.
- (66) Onomura, O.; Arimoto, H.; Matsumura, Y.; Demizu, Y. *Tetrahedron Lett.* **2007**, *48*, 8668–8672.
- (67) Mueller, J. A.; Goller, C. P.; Sigman, M. S. *J. Am. Chem. Soc.* **2004**, *126*, 9724–9734.
- (68) Banik, S. M.; Chung, K.; De Crisci, A. G.; Pearson, D.; Blake, T.; Olsson, J. V.; Waymouth, R. M., submitted for publication.
- (69) Kästele, X.; Klüfers, P.; Kunte, T. Z. *Anorg. Allg. Chem.* **2001**, *626*, 2042–2044.
- (70) Allscher, T.; Kästele, X.; Kettenbach, G.; Klüfers, P.; Kunte, T. *Chem. Asian J.* **2007**, *2*, 1037–1045.
- (71) SAINT and SADABS; Bruker AXS Inc., Madison, WI, 2007.
- (72) Sheldrick, G. M. *Acta Crystallogr., Sect. A* **2008**, *64*, 112–122.
- (73) Müller, P.; Herbst-Immer, R.; Spek, A.; Schneider, T.; Sawaya, M. In *Crystal Structure Refinement: A Crystallographer's Guide to SHELXL*, International Union of Crystallography Texts on Crystallography, 1st ed.; Müller, P., Ed.; Oxford University Press: New York, 2006.
- (74) Smith, M. E. B.; Hibbert, E. G.; Jones, A. B.; Dalby, P. A.; Hailes, H. C. *Adv. Synth. Catal.* **2008**, *350*, 2631–2638.
- (75) Frisch, M. J.; Trucks, G. W.; Schlegel, H. B.; Scuseria, G. E.; Robb, M. A.; Cheeseman, J. R.; Scalmani, G.; Barone, V.; Mennucci, B.; Petersson, G. A.; Nakatsuji, H.; Caricato, M.; Li, X.; Hratchian, H. P.; Izmaylov, A. F.; Bloino, J.; Zheng, G.; Sonnenberg, J. L.; Hada, M.; Ehara, M.; Toyota, K.; Fukuda, R.; Hasegawa, J.; Ishida, M.; Nakajima, T.; Honda, Y.; Kitao, O.; Nakai, H.; Vreven, T.; Montgomery, J. A., Jr.; Peralta, J. E.; Ogliaro, F.; Bearpark, M.; Heyd, J. J.; Brothers, E.; Kudin, K. N.; Staroverov, V. N.; Kobayashi, R.; Normand, J.; Raghavachari, K.; Rendell, A.; Burant, J. C.; Iyengar, S. S.; Tomasi, J.; Cossi, M.; Rega, N.; Millam, J. M.; Klene, M.; Knox, J. E.; Cross, J. B.; Bakken, V.; Adamo, C.; Jaramillo, J.; Gomperts, R.; Stratmann, R. E.; Yazyev, O.; Austin, A. J.; Cammi, R.; Pomelli, C.; Ochterski, J. W.; Martin, R. L.; Morokuma, K.; Zakrzewski, V. G.; Voth, G. A.; Salvador, P.; Dannenberg, J. J.; Dapprich, S.; Daniels, A. D.; Farkas, Ö.; Foresman, J. B.; Ortiz, J. V.; Cioslowski, J.; Fox, D. J. *Gaussian 09, Revision B.01*; Gaussian, Inc., Wallingford, CT, 2009.
- (76) Zhao, Y.; Truhlar, D. G. *Acc. Chem. Res.* **2008**, *41*, 157–167.
- (77) Ditchfield, R.; Hehre, W. J.; Pople, J. A. *J. Chem. Phys.* **1971**, *54*, 724.
- (78) Hehre, W. J.; Ditchfield, R.; Pople, J. A. *J. Chem. Phys.* **1972**, *2257*.
- (79) Hariharan, P. C.; Pople, J. A. *Theor. Chem. Acc.* **1973**, *28*, 213–222.
- (80) Hariharan, P. C.; Pople, J. A. *Mol. Phys.* **1974**, *27*, 209–214.
- (81) Gordon, M. S. *Chem. Phys. Lett.* **1980**, *76*, 163–168.
- (82) Francl, M. M.; Pietro, W. J.; Hehre, W. J.; Binkley, J. S.; DeFrees, D. J.; Pople, J. A.; Gordon, M. S. *J. Chem. Phys.* **1982**, *77*, 3654–3665.
- (83) Binning, R. C., Jr.; Curtiss, L. A. *J. Comput. Chem.* **1990**, *11*, 1206–1216.
- (84) Blaudeau, J.-P.; McGrath, M. P.; Curtiss, L. A.; Radom, L. *J. Chem. Phys.* **1997**, *107*, 5016–5021.
- (85) Rassolov, V. A.; Pople, J. A.; Ratner, M. A.; Windus, T. L. *J. Chem. Phys.* **1998**, *109*, 1223–1229.
- (86) Rassolov, V. A.; Ratner, M. A.; Pople, J. A.; Redfern, P. C.; Curtiss, L. A. *J. Comput. Chem.* **2001**, *22*, 976–984.
- (87) Hay, P. J.; Wadt, W. R. *J. Chem. Phys.* **1985**, *82*, 270.
- (88) Hay, P. J.; Wadt, W. R. *J. Chem. Phys.* **1985**, *82*, 299.
- (89) Roy, L. E.; Hay, P. J.; Martin, R. L. *J. Chem. Theory Comput.* **2008**, *4*, 1029.
- (90) Ehlers, A. W.; Bohme, M.; Dapprich, S.; Gobbi, A.; Hollwarth, A.; Jonas, V. K.; K. F.; Stegmann, R.; Veldkamp, A.; Frenking, G. *Chem. Phys. Lett.* **1993**, *208*, 111.